Immunity
Resource

Systems Scale Interactive Exploration Reveals Quantitative and Qualitative Differences in Response to Influenza and Pneumococcal Vaccines

Gerlinde Obermoser,[1] Scott Presnell,[2] Kelly Domico,[2] Hui Xu,[3] Yuanyuan Wang,[1] Esperanza Anguiano,[1] LuAnn Thompson-Snipes,[1] Rajaram Ranganathan,[1] Brad Zeitner,[2] Anna Bjork,[2] David Anderson,[2] Cate Speake,[2] Emily Ruchaud,[1] Jason Skinner,[1] Laia Alsina,[1] Mamta Sharma,[1] Helene Dutartre,[1] Alma Cepika,[1] Elisabeth Israelsson,[2] Phuong Nguyen,[1] Quynh-Anh Nguyen,[1] A. Carson Harrod,[1] Sandra M. Zurawski,[1] Virginia Pascual,[1] Hideki Ueno,[1] Gerald T. Nepom,[2] Charlie Quinn,[1,2] Derek Blankenship,[3] Karolina Palucka,[1,*] Jacques Banchereau,[1] and Damien Chaussabel[1,2,*]

[1]Baylor Institute for Immunology Research, Baylor Research Institute, Dallas, TX 75204, USA
[2]Benaroya Research Institute, Seattle, WA 98101, USA
[3]Baylor Institute for Health Care Research and Improvement, Dallas, TX 75206, USA
*Correspondence: karolinp@baylorhealth.edu (K.P.), dchaussabel@benaroyaresearch.org (D.C.)
http://dx.doi.org/10.1016/j.immuni.2012.12.008

SUMMARY

Systems immunology approaches were employed to investigate innate and adaptive immune responses to influenza and pneumococcal vaccines. These two non-live vaccines show different magnitudes of transcriptional responses at different time points after vaccination. Software solutions were developed to explore correlates of vaccine efficacy measured as antibody titers at day 28. These enabled a further dissection of transcriptional responses. Thus, the innate response, measured within hours in the peripheral blood, was dominated by an interferon transcriptional signature after influenza vaccination and by an inflammation signature after pneumococcal vaccination. Day 7 plasmablast responses induced by both vaccines was more pronounced after pneumococcal vaccination. Together, these results suggest that comparing global immune responses elicited by different vaccines will be critical to our understanding of the immune mechanisms underpinning successful vaccination.

INTRODUCTION

Vaccines represent one of the greatest achievements of medicine because they can elicit specific and durable protective immune response. Most, if not all, preventive vaccines are designed to initiate protective humoral immune responses. In the United States alone, over 70 vaccines are currently licensed (FDA, 2011). Surprisingly, very little is known about the immunological mechanisms underpinning the development of the protective immune responses elicited by these vaccines. Profiling blood transcript abundance on a systems scale has been successfully implemented to investigate disease pathogenesis (Alakulppi et al., 2008; Bennett et al., 2003; Pascual et al., 2010; Ramilo et al., 2007; Tang et al., 2009) and, more recently, responses to vaccines and adjuvants (Bucasas et al., 2011; Caskey et al., 2011; Gaucher et al., 2008; Mallory et al., 2010; Nakaya et al., 2011; Querec et al., 2009). The distinct advantage of a "systems approach" is that it is unbiased (i.e., it does not require a priori selection of the parameters that will be measured but instead encompasses the entire available repertoire—the human genome). Other large-scale profiling technologies, such as multiparameter flow cytometry or multiplex serum protein assays complete the systems immunology armamentarium, providing unprecedented capabilities to characterize the human immune response (Germain et al., 2011; Maecker et al., 2012).

The volume of data being generated by such approaches is also unprecedented. With the robustness and cost effectiveness of high-throughput profiling platforms improving constantly, the trend is expected to accelerate in the coming years. The challenges posed by this sudden overabundance of data are many: from data storage and management to integration, analysis, and interpretation (Chaussabel et al., 2009; Germain et al., 2011). Also crucial is an effective means of communicating and disseminating this wealth of information, especially for investigators with limited bioinformatics expertise. Indeed, the usefulness of large-scale data sets can be extended well beyond the publication of study results by presenting data in a manner that promotes insight and supports further knowledge discovery. Providing seamless access to the primary data underlying the analysis results should also improve transparency and build confidence in the conclusions of a study.

Here, we investigated two widely used vaccines, both of which induce protective antibody responses. The trivalent influenza vaccine is composed of three chemically inactivated influenza A and B virus strains (split virus vaccine), whereas the 23-valent pneumococcal vaccine consists of polysaccharide extracts from the 23 most common disease-causing serotypes of *Pneumococcus pneumoniae*. We used high-throughput profiling technologies to measure perturbations that occur in the blood at the molecular and cellular levels in vivo. By adopting a comparative approach, we show that these two vaccines elicit common, as well as distinct, transcriptional signatures, both early (innate immunity) and late (adaptive immunity), that

eventually lead to the development of protective antibody responses. Interactive versions of the figures presented throughout this paper provide readers with the opportunity to access the underlying data presented. Furthermore, a portal is provided to allow the dynamic investigation of the entirety of the data generated in the context of this study. Finally, insight gained through data exploration can be gathered, organized, and shared via integrated email and social networking applications.

RESULTS

Influenza and Pneumococcal Vaccines Elicit Changes in Blood Transcript Abundance

Young, healthy, adult volunteers were recruited and randomly assigned to three study groups receiving either 2009–2010 seasonal influenza vaccine (Fluzone®), 23-valent pneumococcal vaccine (Pneumovax23®), or saline injections. Blood samples were collected by venipuncture at days −7, 0, 1, 3, 7, 10, 14, 21, and 28 (see Tables S1 and S2 available online). Neutralizing antibody titers elicited by the different vaccines were determined at days 0 and 28 and demonstrated seroconversion in the majority of subjects (Tables S3 and S4; Figure S1).

Vaccine responses were assessed through the analysis of global changes in transcript abundance in whole blood samples. Whole-genome transcriptional profiles were generated at each time point from the first cohort of volunteers (n = 6 subjects/group; 162 samples in total). Specific time points where significant differences were found in comparison to baseline for each group (false discovery rate [FDR] = 0.10) were identified. Of the 3,102 transcripts for which abundance was significantly altered in response to vaccines, 239 changed by more than 2-fold in at least one time point. Patterns of transcript abundance across all samples for this robust set are represented on a heatmap (Figure 1A). In addition, a circular plot was generated where segments forming the perimeter correspond to differentially expressed gene lists (Figure 1B). Differentially expressed gene lists for each group combining all time points and for each time point combining all the groups are shown on this graph. The length of each segment is proportional to the number of genes constituting the list. It is thus possible to visualize that the number of responsive genes was the largest for the pneumococcal vaccine group and the smallest for the saline control group. Among the different time points, the majority of the changes were seen at days 1 and 7. Connections between the segments representing the groups (right) and those representing the time points (left) indicate how differentially expressed genes for a given group are distributed across the different time points and, conversely, how genes for a given time point are distributed across the different groups. An interactive version of this figure can be used to explore lists of differentially expressed genes (http://www.interactivefigures.com/dm3/circleChart/arcCirclePlot). This reveals, for instance, that most of the genes shown at day 7 and all of the genes at day 10 are induced by pneumococcal vaccination. It also shows both influenza and pneumococcal vaccines induce robust responses at day 1 postvaccination. This initial analysis indicates substantial changes in blood transcript abundance can be detected in response to these two non-live vaccines.

Changes in Transcript Abundance Are Detected at the Module Level 1 and 7 Days Postvaccination

We next sought to gain additional insight about the nature of those vaccine-elicited responses. A modular repertoire analysis was performed relying on coordinately expressed gene sets, also called modules. These modules are constructed via an entirely data-driven process of recapitulating fluctuations in blood transcript abundance measured across a wide range of diseases (as described previously [Chaussabel et al., 2008]) and detailed in Supplemental Experimental Procedures. Modules are thoroughly annotated (http://www.biir.net/public_wikis/module_annotation/V2_Trial_8_Modules) and constitute a simplified framework for the analysis of blood transcriptome data.

The first step consisted in determining for each module the proportion of transcripts for which abundance was significantly changed in comparison to prevaccine levels. A module is considered to be "responsive" to vaccination when the proportion of significant transcripts is greater that what could be expected by chance (FDR = 0.10). Out of 62 modules, 17 and 14 passed this threshold at day 1 in the influenza vaccine and pneumococcal vaccine groups, respectively (Figure 2A). Subsequently, changes in transcript abundance were detected for 3 modules and 1 module at day 7 and 10, respectively, in the pneumococcal vaccine group and for a single module at day 7 and day 21 in the influenza vaccine group (Figure 2A). Thus, these two vaccines show different magnitudes of transcriptional responses at different time points after vaccination.

Module-Level Exploration of the Innate Responses to Pneumococcal and Influenza Vaccines

The day 1 responsive modules were mapped on a grid where each position corresponds to one of the 62 modules used in this analysis. A colored spot indicates the proportion of significant transcripts for a given module. When transcript abundance for the module increases over the prevaccination levels, the spot is red; when transcript abundance decreases, it is blue. This visualization scheme reveals important qualitative differences between responses elicited by the influenza and pneumococcal vaccines (Figure 2B).

These figures can be explored via interactive web supplements (http://www.interactivefigures.com/dm3/vaccine-paper/figure-2.gsp). "Drill down" functionalities provide users with access to source gene-level data that are integrated with other data types (clinical information, multiplex cytokine analysis, and flow cytometry data). In addition, Wiki media was leveraged to provide access to extensive functional analysis results for each module. Finally, stringency level of the analysis can be changed dynamically to assess the robustness of the changes measured in response to vaccines. A short video tutorial is available to demonstrate available functionalities.

Influenza and Pneumococcal Vaccines Elicit Distinct Innate Immune Responses

Changes in eight modules were common to both vaccines, including increased modules M4.6 (functionally associated with inflammation), M6.6 and M6.13 (apoptosis/cell death) and decreased modules M4.1 and M4.15 (T cells), M4.3 (protein synthesis), M5.11, and M6.9 (no functional annotation).

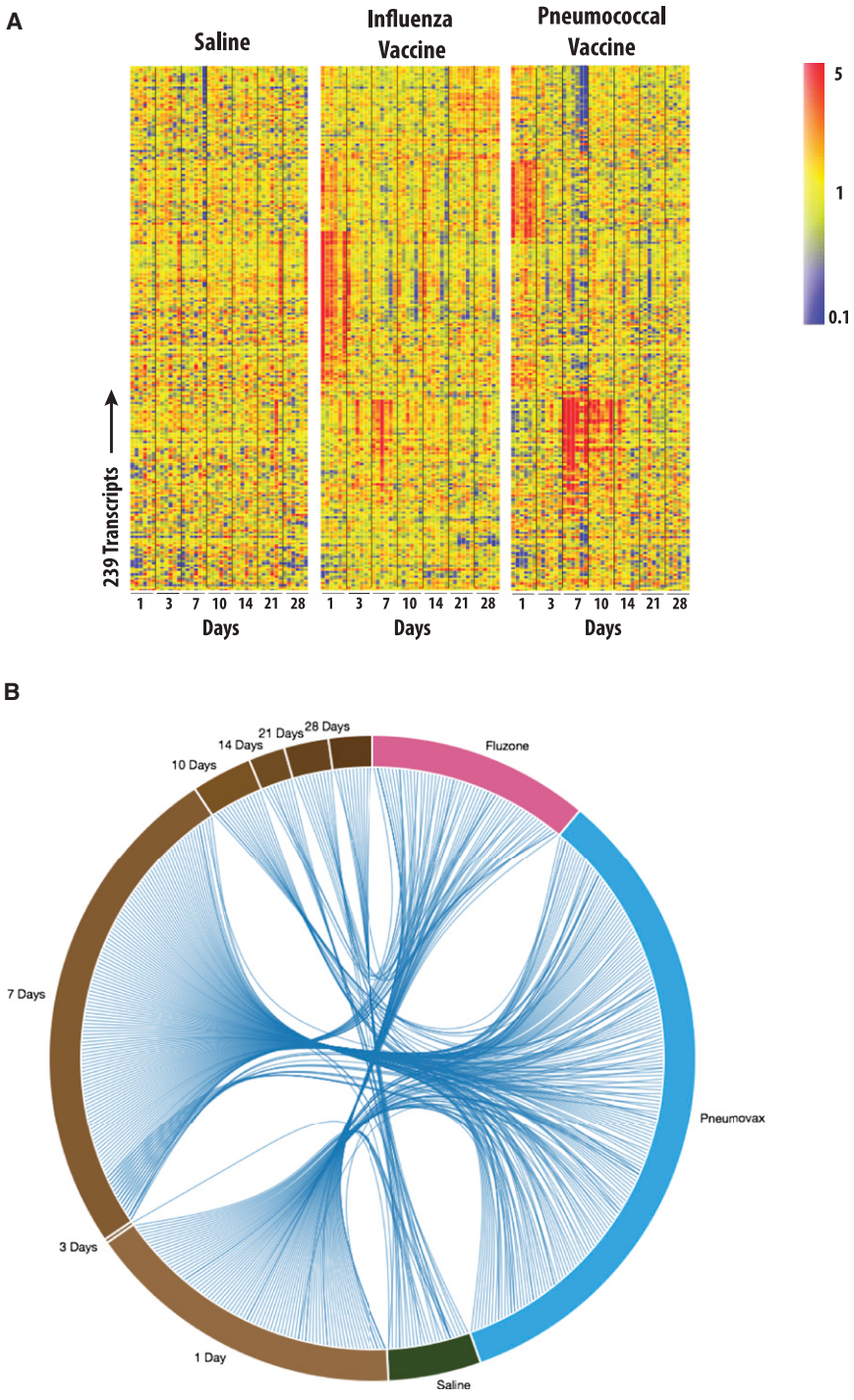

Figure 1. Blood Transcriptional Profiles of Vaccinated Subjects

(A) Patterns of changes in transcript abundance are shown on a heatmap for a robust set of 239 transcripts using an FDR of 0.10 and fold change >2). For each subject, data are normalized to the average of the two baseline time points. Red represents relative increase in abundance, blue represents relative decrease, and yellow represents no change.

(B) Lists of genes differentially expressed in response to each treatment for all time points or at each time point for all treatments are represented as segments on a circle. The length of the segments is proportional to the number of genes in each list. A link between two segments on this circular plot indicates an overlap between two gene lists between treatments (segments on the right) and time points (segments on the left). An interactive supplement is available for this figure that dynamically highlights how shared genes of one segment are distributed across all other segments and displays symbols for the corresponding genes (iFigure 1B: http://www.interactivefigures.com/dm3/circleChart/arcCirclePlot). It also provides the user with the ability to dynamically add a cutoff based on fold-change expression over baseline and to adjust the aspect of the graph. For study design, see Figure S2 and Tables S1, S2, and S5; for comparison of transcriptional profiles across cohorts, see Figure S3.

Nine modules were uniquely responsive to the influenza vaccine. Of those, four were significantly increased and five were significantly decreased (Figure 3A; http://www.interactivefigures.com/dm3/vaccine-paper/figure-3.gsp). Three of the four increased modules were associated with antiviral responses (M1.2, M3.4, M5.12, Ingenuity Pathway Analysis enrichment p values) and included many genes coding for prototypical interferon (IFN)-inducible antiviral molecules such as OAS1, OAS2, OASL (M1.2); Guanylate Binding Proteins GBP1, GBP2, GBP4, GBP6 (M3.4); and TRIM family members such as TRIM5, TRIM21, TRIM25, TRIM38, TRIM56 (M5.12). The fourth increased module, M4.14, was associated with myeloid lineage and monocytes and includes, among others, genes coding for CD97, CD1D, interleukin-6 (IL-6), LY86, and CSF1R. Modules that were decreased include M3.6 (natural killer cells and cytotoxicity), M4.7 (cell cycle), and three modules without definitive functional annotation (M4.8, M5.8, and M6.15).

Six modules were uniquely responsive to the pneumococcal vaccine. Of these, five were modules including genes associated with inflammation (Figure 3B): M3.2 (e.g., CD63, IL-1RN, HMGB2, TLR4, TLR6, TLR8, as well as bcl-6), M4.2 (e.g., CR1, MMP9, TLR5), M4.13 (e.g., CD58, IL-8RA, CXCL1, and IL-1β), and M5.1 (e.g., CCR1, SERPINB8, MAPK1) and M5.7. Only one module, M4.12 (not annotated), was decreased. These day 1 signatures obtained in the first cohort of subjects were subsequently validated in two independent cohorts of subjects (Figure S2). There, normalized expression values of individual transcripts were averaged for each responsive module. Average values obtained for cohorts 1, 2, and 3 were significantly correlated (Pearson correlation, $p < 0.001$, $n = 5–6$ subjects per group, Figure S3). These module-based results

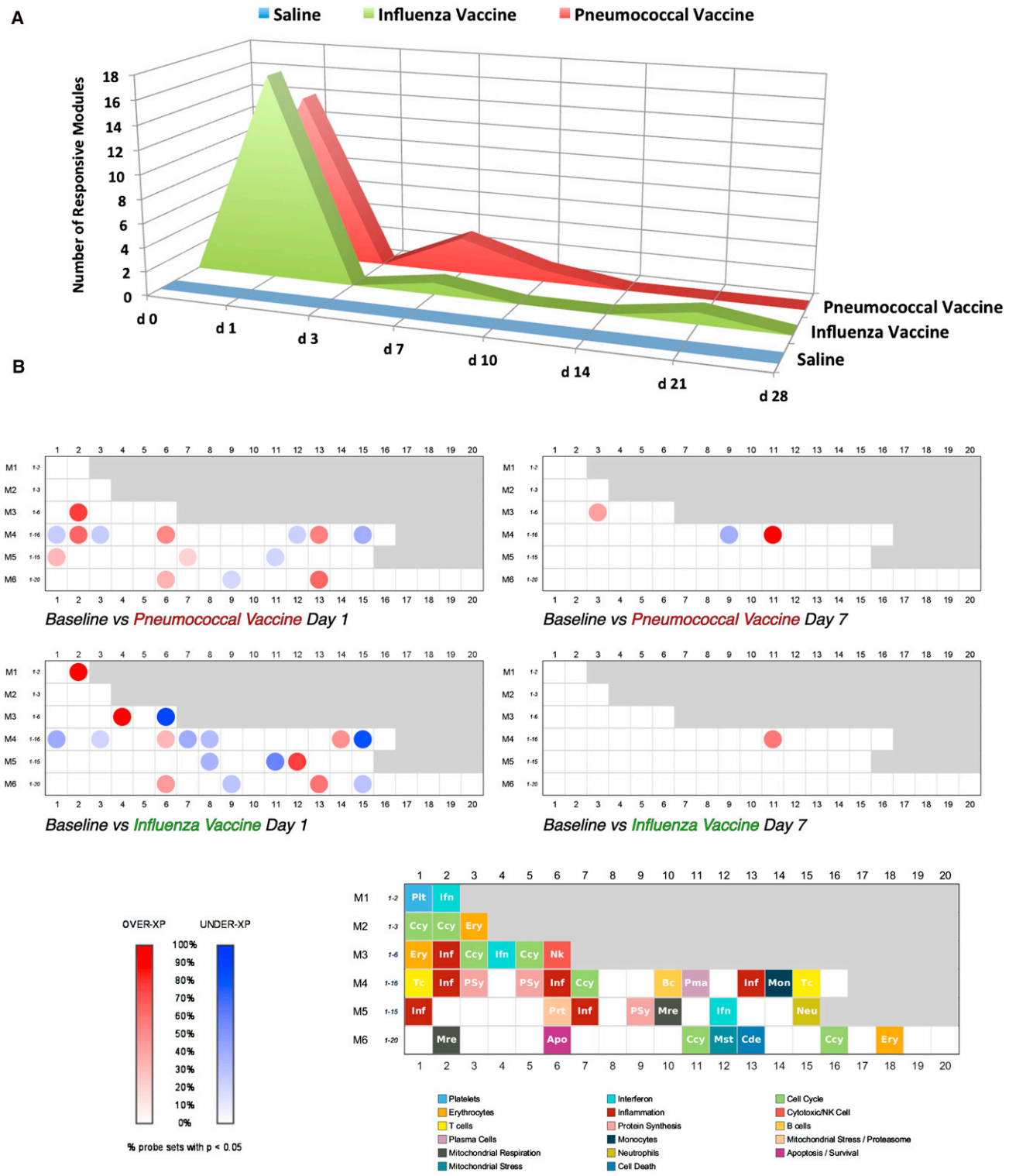

Figure 2. Modular Mapping of the Global Changes in Blood Transcript Abundance Elicited by Vaccination

Changes in transcript abundance measured in blood by using whole-genome arrays were mapped against a preconstructed modular analysis framework. The proportion of transcripts for which abundance was significantly changed in comparison to prevaccination levels was determined for each module. When this proportion exceeded the false discovery rate (set at 10%), the module was considered to be responsive to treatment.

(A) The number of responsive modules is plotted on a graph at each time point for all three of the treatment groups.

(B) Responsive modules are mapped on a grid for the two vaccine groups at days 1 and 7. The proportion of significant transcripts for each module is represented by a spot of color, with red representing increased abundance and blue representing decreased abundance. The position on the grid indicates the round and

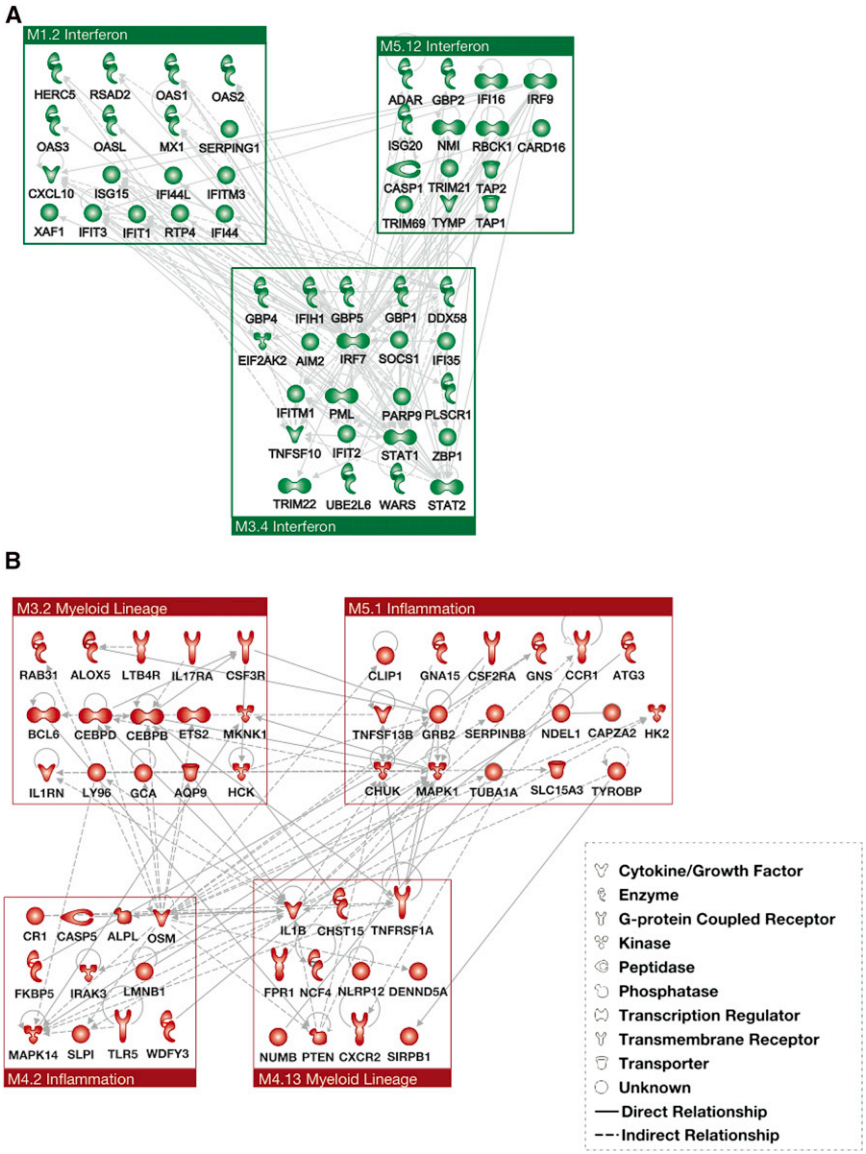

Figure 3. Functional Interpretation of Influenza and Pneumococcal Vaccine Day 1 Signatures

Modules specifically responsive to the influenza (A) or pneumococcal (B) vaccines were subjected to pathway analysis. Only the genes within each module for which transcript abundance was significantly changed following vaccination were included in this analysis. Genes with at least one connection (indicating for instance protein-protein interaction or regulation) are represented in this figure. An interactive supplement for this figure provides access to the entire list of genes that constitute each module and to extensive functional annotations (iFigure 3: http://www.interactivefigures.com/dm3/vaccine-paper/figure-3.gsp).

demonstrate how each vaccine elicits a distinct innate immune response.

Changes in Blood Transcript Abundance Are Detected within Hours following Vaccine Administration

To further analyze the kinetics of the innate response to vaccination, we generated whole-genome transcriptional profiles from blood collected within hours following vaccine or saline administration in an independent patient cohort (n = 6 subjects per group). Blood samples were collected via finger stick at hours –168, 0, 1.5, 3, 6, 9, 12, 15, 24, 36, and 48, for whole-genome transcriptional profiling (198 samples in total) (see Table S5). Changes in transcript abundance at each time point postvaccination were identified as described above. To characterize the nature of the evolving innate immune response, we systematically compared these signatures with gene-expression profiles induced by in vitro culture of blood with a wide range of Toll-like receptor (TLR) agonists and cytokines. The concordance between in vivo and in vitro signatures is shown by using circular plots (Figure 4; http://www.interactivefigures.com/dm3/vaccine-paper/figure-4.gsp). There, the degree of connectivity between the various segments on the plot indicates the degree of overlap between the in vivo- and in vitro-derived gene lists. The signature elicited within hours following immunization with seasonal influenza vaccine overlapped with transcripts induced by a small set of innate immune stimuli including heat-inactivated gram-negative bacteria, heat-inactivated viruses (RSV, influenza), and IFN-γ. The overlapping gene transcript set was dominated by interferon-inducible genes, including the transcription factor EGR1, ADAR (RNA-editing enzyme that deaminates adenosines and modifies viral genomes), Fcγ receptors, GBP1 and GBP2 (IFN-inducible, specifically bind guanine nucleotides), IFI16 (amplifier in intracellular DNA recognition response), HLX (transcription factor involved in T helper 1 cell (Th1)-type response polarization), IRF1 and IRF9 (transcription factors involved in type I IFN production and IFN signaling), STAT1 (transcription factor that mediates the IFN response), TAP1 (involved in antigen presentation via MHCI), TLR7

order of selection. For instance, the fourth module of the third round of selection (M3.4) is situated in the fourth column, third row. The degree of intensity of the spots denotes the percentage of significant transcripts. A legend is provided with functional interpretations indicated at each position of the grid by a color code. An interactive supplement is available for this figure that provides access to gene level data and extensive functional annotations for each module. The interactive figure also allows users to dynamically adjust the stringency of the analysis (iFigure 2B: http://www.interactivefigures.com/dm3/vaccine-paper/figure-2.gsp).

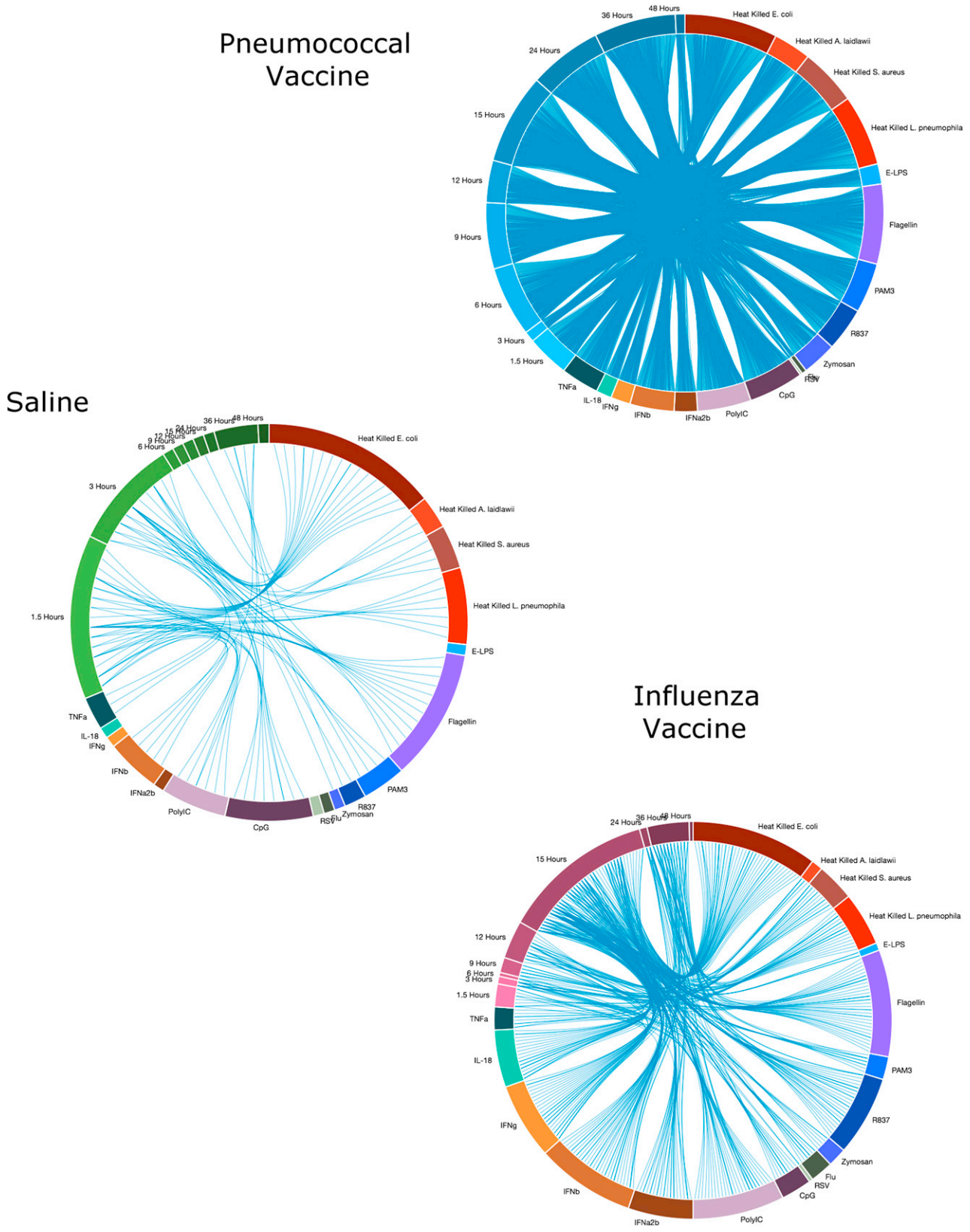

(legend on next page)

(receptor for single stranded RNA) and TRAIL (TNFSF10, involved in induction of apoptosis). The pneumococcal vaccine signature overlapped with in vitro signature induced by heat-inactivated bacteria, LPS, flagellin, PAM3, R837, zymosan, CpG, IFN-γ, IL-18. The overlapping gene transcript set included IL-1B, IL-1RN, IL-6R, ADM (a vasodilatator), FCGR2A, TRAIL and CASP4 (apoptosis inducers), IRF2 (inhibits IRF1-mediated IFN induction and binds to the IL7 promoter), and transcription factors BCL3 (NF-κB signaling), VAV1 (Rho signaling), BCL6, and ETS2 (leukocyte differentiation and/or proliferation). The gene lists obtained for the control saline group were only sparsely connected. This analysis demonstrates that vaccines act as potent activators of the innate immune system and that responses can be detected in the blood in vivo within hours following administration. The interactive online figure allows further exploration of the circular plots, giving readers the ability to dynamically display lists of overlapping genes and change the stringency of the filters (Figure 4; http://www.interactivefigures.com/dm3/vaccine-paper/figure-4.gsp).

A Modular Interferon Signature Is Detected 15 hr following Influenza Vaccination

To complement observations made at the gene level, we next analyzed early transcriptional responses to vaccines at the module level. Baseline-normalized values for each gene within a module were averaged. We decided to focus on IFN-inducible modules and to further investigate the kinetics of induction by the influenza vaccine (M1.2 shown on Figure 5A and with each point linked to detailed sample information in http://www.interactivefigures.com/dm3/vaccine-paper/figure-5.gsp). Significant changes in the transcription of genes forming IFN response module were observed as early as 15 hr following administration of the vaccine and persisted to 48 hr postvaccination.

Next, the contributions were determined for different leukocyte populations to this interferon signature. To this end, we isolated neutrophils, monocytes, and $CD4^+$ and $CD8^+$ T cells from the blood of study subjects before and 24 hr after the administration of the influenza vaccine (n = 6) in a third sequential cohort of healthy subjects (48 samples in total). The analysis revealed differences in the levels of expression for IFN-inducible transcripts in neutrophils and in monocytes following influenza vaccination (module-level data shown in Figure 5B; http://www.interactivefigures.com/dm3/vaccine-paper/figure-5.gsp). Furthermore, serum levels of the IFN-inducible chemokine CXCL10 (IP-10) were also found to increase significantly on day 1 after influenza vaccination ($p < 0.01$; Figure S4).

Thus, administration of the influenza vaccine leads to early type I interferon signature in the blood carried by neutrophils and monocytes.

Pneumococcal Vaccine Elicits a Prominent Plasmablast Signature on Day 7

We next analyzed modular transcriptional responses at later time points after vaccine administration. Day 7 samples demonstrated changes in the abundance of transcripts constituting module M4.11 in both the influenza and pneumococcal vaccine groups (Figure 2B). This module includes genes encoding CD38, IGJ, TNFRSF17 (BCMA), TXNDC5, GLDC, CAMK1G, and immunoglobulin kappa chains and constitutes a plasma cell precursor signature. At day 7, the abundance of 35% of the transcripts forming module M4.11 increased significantly in comparison to prevaccination levels in the influenza vaccine group. In the pneumococcal vaccine group, 70% of the M4.11 transcripts were significantly increased. Furthermore, the amplitude of the plasma cell precursor signature induced by pneumococcal vaccination was significantly greater than that induced by influenza vaccination at both days 7 and 10. As described above, baseline-normalized values for each gene within a module were averaged and plotted on a graph (Figure 6A; http://www.interactivefigures.com/dm3/vaccine-paper/figure-6.gsp). These results were reproduced in our validation cohort (cohort 2, n = 6 subjects per group). Two other modules, M3.3 and M4.9, were responsive to pneumococcal vaccination only at day 7 (data not shown). Genes from M3.3 code for molecules involved in cell cycle and replication, including a number of cyclins, kinesins, and centromere proteins; functionally, M3.3 is associated with hematopoiesis. Module M4.9 includes molecules involved in leukocyte extravasation (ACTG1, CXCR4, CDC42, CRK, ROCK1, and RASSF5). These findings at the transcriptional level are in line with changes in cellular composition showing a spike in circulating plasmablasts at day 7 after vaccination. Plasmablasts were identified by polychromatic flow cytometry in whole blood samples as $CD19^{+/lo}CD20^{-}CD27^{+}CD38^{hi}$ plasmablasts and plasma cells. Figure 6B shows the kinetics of changes in the absolute numbers of $CD19^+$ B cells and plasmablasts over time after vaccination. There, 11-fold and 47-fold increases in the absolute numbers of plasmablasts were observed following vaccination with influenza and pneumococcal vaccines, respectively. The peak levels reached a mean of 8.5 cells/uL and 71.7 cells/uL in response to influenza and pneumococcal vaccines, respectively. This increase was significant at day 7 following administration of the influenza vaccine and on days 7 and 10 following administration of the pneumococcal vaccine. The interactive figure provides access to the flow cytometry pseudocolor dot plots that show the composition of the B cell compartment (Figure 6B; http://www.interactivefigures.com/dm3/vaccine-paper/figure-6.gsp). Consistent with transcriptional profiles, both vaccines lead to expansion of plasmablasts and/or plasma cells with a much greater expansion observed after pneumococcal vaccine (range: 11.4%–35.9% versus

Figure 4. Mapping of the Response to Vaccines In Vivo and the Response to Innate Immune Ligands In Vitro

Lists of genes differentially expressed at nine consecutive time points post vaccine administration or following in vitro treatment of blood for 6 hr with a wide range of innate stimuli are represented as segments of a circle. The lengths of the segments are proportional to the number of genes in each list. A link between two segments on this circular plot indicates an overlap between two gene lists. The degree of connectivity between the various segments on this plot indicates the degree of overlap between in vivo- and in vitro-derived gene lists. An interactive supplement is available for this figure. Overlapping genes are listed when segments are selected. The tension of lines and stringency of the filters (fold change and p value slider) can be adjusted dynamically. For computation of the p value slider, baseline and time point microarray data were used in paired t tests. For each paired in vitro/in vivo gene, the greater p value of the pair is used in the p value filter (iFigure 4: http://www.interactivefigures.com/dm3/vaccine-paper/figure-4.gsp).

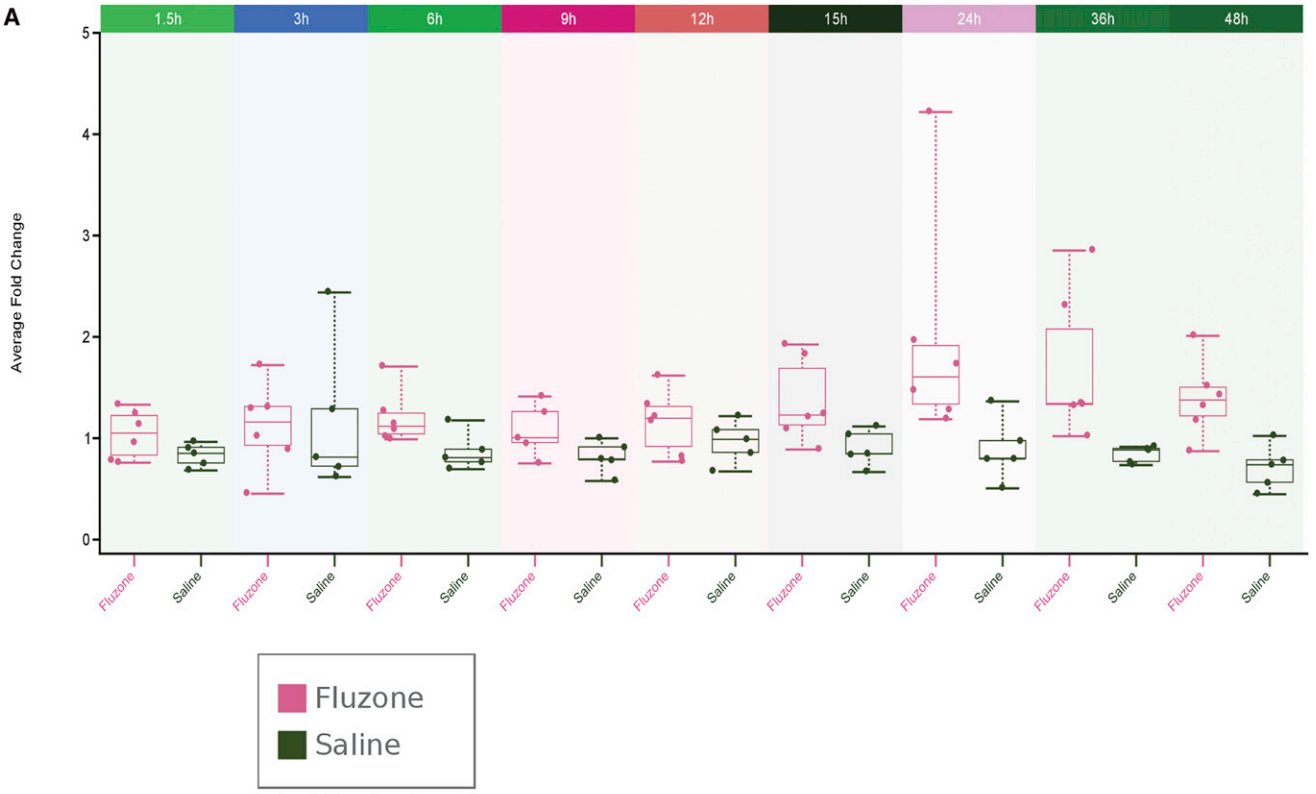

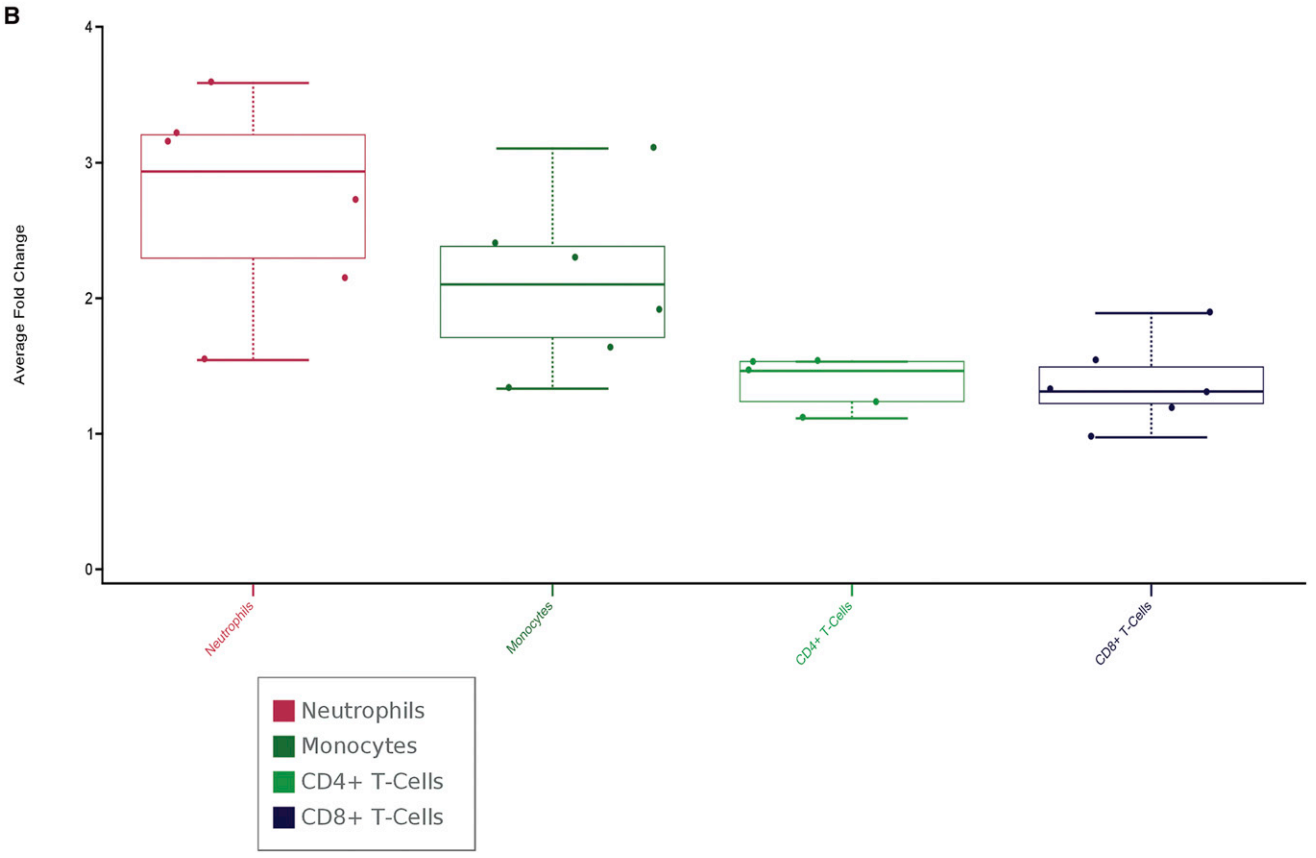

(legend on next page)

27.9%–86.2%, respectively). Thus, blood transcriptional profiling and flow cytometry reveal qualitative and quantitative differences in adaptive immune responses to these two vaccines with pneumococcal vaccine generating larger and longer lasting plasmablast responses.

Exploring Correlation Patterns Predictive of Vaccine Response

Mining of large-scale immune profiling data can yield critical insight into factors determinant of effective vaccination. We explored correlations between day 1 and day 7 modular fingerprints and increases in antibody levels for all available serotypes, combining results from all available subjects for both vaccination groups. The strongest correlations were observed between day 7 modular transcriptional data and serology results in the pneumococcal vaccine group. The strongest positive correlations were found for modules M3.3 (annotated as cell cycle) and M4.11 (plasma cells) and to a lesser extent M4.10 (B cells), M5.10 and M6.2 (both associated with mitochondrial respiration). Strong negative correlations were observed at the same time point for modules associated with inflammation (M3.2, M4.2, and M4.13). Showing correlation (r) values in a heatmap format revealed a high degree of consistency in these correlations across all serotypes (Figure 7A). In contrast, correlation patterns observed between day 7 modular transcriptional data and serology results in the influenza vaccine group were more varied for the different virus strains tested. The vaccine used in this study (2009/10 Fluzone from Sanofi Pasteur) contained inactivated A/Brisbane/59/2007 IVR-148 (H1N1), A/Uruguay/716/2007 NYMC X-175C (H3N2) (an A/Brisbane/10/2007 H3N2-like virus), and B/Brisbane/60/2008 strains. Some day 7 modules correlating to levels of antibodies were similar to those found in the pneumococcal vaccine group (M4.11 and M4.10) (Figure 7B) with B Brisbane showing the strongest positive correlation with M4.11 and an increase in HAI titers ($r = 0.77$). Levels of antibodies against the Brisbane H3N2 strain were inversely correlated with M3.3 (cell cycle) in contrast to a positive correlation for B Brisbane and Brisbane H1N1 strains. Correlation patterns were also observed in day 1 influenza vaccine modular signatures, which showed positive correlations of IFN modules M1.2, 3.4, and M5.12 (http://www.interactivefigures.com/dm3/vaccine-paper/figure-7.gsp). Although independent validation of these findings will be required, these results highlight the value of using unbiased exploratory approaches toward identification of determinants of successful vaccine responses.

DISCUSSION

We demonstrate that different vaccines against infectious agents elicit different transcriptional and cellular responses in the blood. Indeed, both seasonal influenza and pneumococcal vaccines showed a spike in transcriptional activity within 24 hr after intramuscular administration, suggesting activation of the innate immune system. However, there were important qualitative differences in the transcriptional profiles. Whereas the pneumococcal vaccine induced an increase in abundance of myeloid- and inflammation-related gene transcripts, the influenza vaccine produced an IFN-inducible transcriptional signature at day 1 after vaccination. Neither vaccine includes an adjuvant, but they differ fundamentally in their composition. The seasonal influenza vaccine is composed of inactivated virus particles, whereas the pneumococcal vaccine is composed of a mix of polysaccharides. Thus, different vaccines might lead to development of adaptive immunity through different innate immune pathways. However, a mechanism common to both vaccines is also at play as demonstrated by the shared transcriptional profiles at day 1 that we observed for 8 modules, including upregulation of modules related to myeloid lineage and inflammation.

To investigate the kinetics of the early innate vaccine response, we collected blood by a finger prick and by using transcriptional profiling detected the upregulation of IFN-inducible genes as early as 15 hr after vaccine administration. In line with our observations, Bucasas et al. reported for the 2008–2009 seasonal influenza vaccine upregulated expression of interferon signaling genes like STAT1 and IRF9 in the blood on day 1 after vaccination (Bucasas et al., 2011). Although the study by Nakaya et al. did not include collection of blood samples on day 1 after vaccination, this group reported on a signature of IFN-related genes in purified blood mononuclear cells (rather than whole blood) on day 3, thus correlating with the serological response to vaccination with inactivated influenza vaccine (Nakaya et al., 2011).

We went further and isolated neutrophils, monocytes, and $CD4^+$ and $CD8^+$ T lymphocytes from peripheral blood before and 1 day after vaccination. This analysis revealed that neutrophils and monocytes are the main cellular source of the day 1 influenza vaccine interferon signature in the blood. Interestingly, we have recently identified a similar neutrophil- and monocyte-driven blood interferon signature correlating with disease severity in patients with tuberculosis (Berry et al., 2010).

At day 7 after vaccination, we found plasmablast-related gene transcriptional activity consistent with a generation of adaptive immune responses, confirmed by detection of humoral immune responses at day 28 (as shown by serology). Transcripts include genes such as CD38 or TNFRSF17 (BCMA), one of the receptors of BlyS-BAFF, which have previously been described as part of a day 7 peripheral blood mononuclear cell (PBMC) signature predictive of the neutralizing antibody response to yellow fever vaccination and (inactivated) seasonal influenza vaccine (Nakaya et al., 2011; Querec et al., 2009). A burst in circulating

Figure 5. Profiling the Interferon Response within the First 48 hr following Vaccination

(A) Baseline-normalized whole-blood expression levels of genes forming module M1.2 (IFN-inducible gene module) were averaged and plotted on a graph. Values are shown at multiple consecutive time points for the influenza vaccine and saline control groups. For concomitant serum increase of IFN-inducible chemokine CXCL10 (IP-10), see Figure S4.

(B) Baseline-normalized expression levels of genes forming module M1.2 were averaged and plotted on a graph. Values are shown for different cell populations isolated from the blood of subjects 24 hr postvaccination. Box plots with whiskers indicating minimum and maximum value. An interactive supplement is available for this figure, where detailed sample information is accessible seamlessly for each data point on the graph (iFigure 5: http://www.interactivefigures.com/dm3/vaccine-paper/figure-5.gsp).

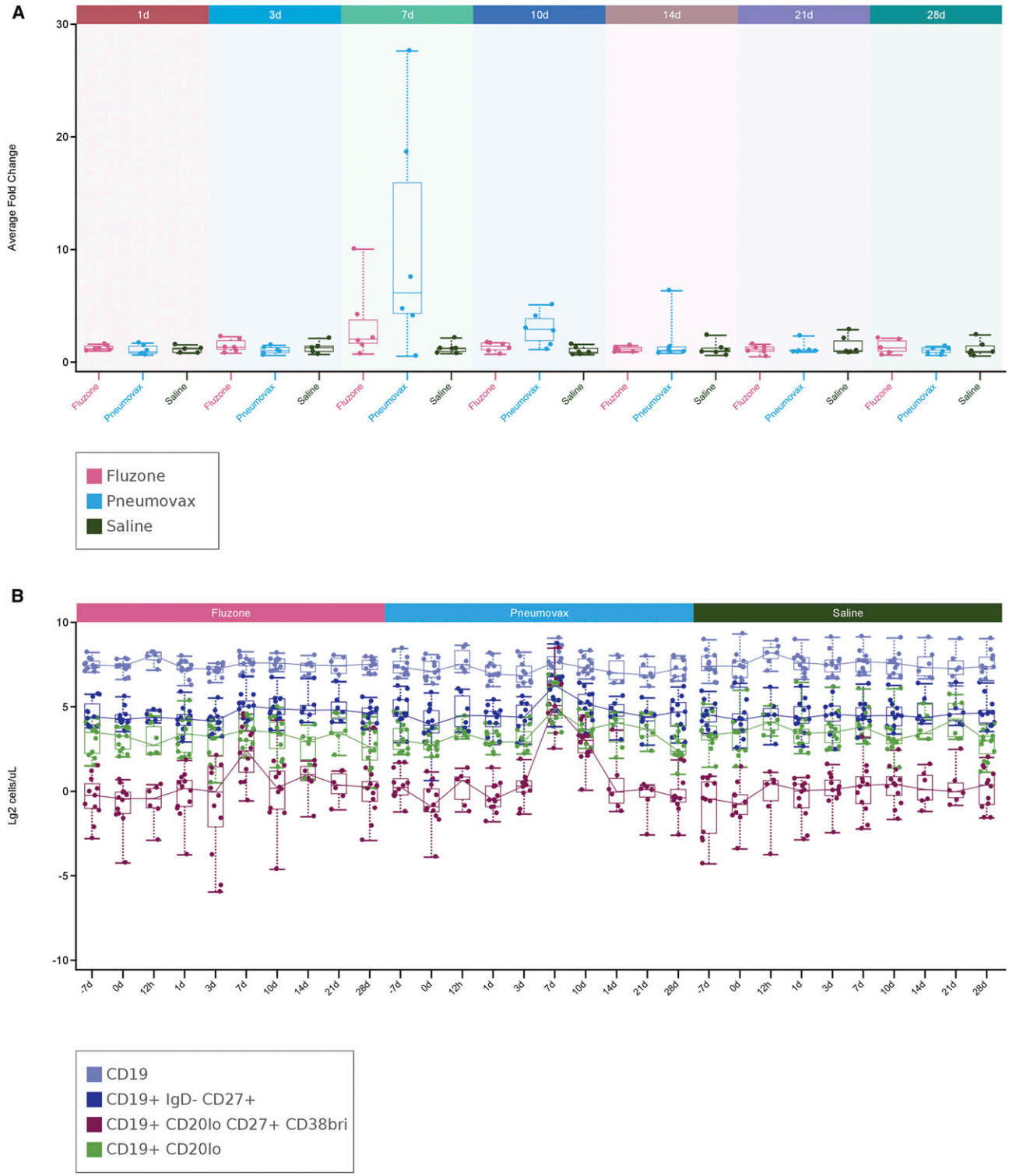

Figure 6. Plasma Cell Precursor Immune Signature

(A) Baseline-normalized whole blood expression levels of genes forming module M4.11 (plasma cell precursors module) were averaged and plotted on a graph. Values are shown at multiple consecutive time points for the influenza vaccine, pneumococcal vaccine and saline control groups.

(B) Abundance of plasmablasts measured by multi-parameter flow cytometry is plotted on a graph. Values are shown at multiple consecutive time points for the influenza vaccine, pneumococcal vaccine and saline control groups. Box plots with whiskers indicating minimum and maximum value. An interactive supplement is available for this figure where detailed sample information including dot plots for flow cytometry measurements is seamlessly accessible for each data point on the graph (iFigure 6: http://www.interactivefigures.com/dm3/vaccine-paper/figure-6.gsp).

plasmablasts was concomitantly observed at day 7 by flow cytometry. This is consistent with recent studies by Nakaya et al. (2011) and Querec et al. (2009) and suggests the development of adaptive immune responses. Indeed, Wrammert et al. showed that up to 85% of plasmablasts purified at the peak of response can be influenza-vaccine-specific, pauciclonal, and producing mainly immunoglobulin G (IgG) of highest affinity (Wrammert et al., 2008).

Two studies recently reported a correlation between day 1 or day 3 upregulated genes involved in IFN signaling and the magnitude of the antibody response (Bucasas et al., 2011; Nakaya et al., 2011). Exploratory analysis of correlation patterns in the influenza vaccine group showed a correlation of day 1 module M5.12 (IFN) expression and serological response to Brisbane H1N1 ($r = 0.66$) and of day 7 M4.11 (plasma cells) with serological response to B Brisbane vaccine strain ($r = 0.77$). Likewise, day 7 module M4.11, as well as M4.10 (B cells), correlated with serological response. Together, these results suggest that comparing global immune responses elicited by different vaccines will be critical to our understanding of the immune mechanisms underpinning successful vaccination.

An important goal of this work was to implement means to extend the value of data generated by using systems immunology approaches beyond publication of the results. Therefore, we developed web applications to allow mining and interpretation of the data by other investigators. In addition to interactive figures, we developed a data portal allowing users to dynamically query and graph the primary data generated in this study (http://www.interactivefigures.com/dm3/vaccine-paper/portal-landing.gsp). There, profiles of individual genes can be plotted and integrated with any clinical or immunological data with a user-friendly data browsing application (http://www.interactivefigures.com/dm3/flash/vaccine-paper-dataportal/iFig_dataportal.html). We have also integrated features that facilitate the harvesting and dissemination of findings that investigators discover while browsing the data. All images and underlying data are downloadable and web links that record a specific view of the data can be shared by email directly from the application. We also leveraged social networking media to facilitate sharing of these findings (http://www.interactivefigures.com/dm3/flash/vaccine-paper-gplusfig/gPlusFig.html). Registered Google+ users can, at the click of a button, post web links and images from our application, along with personal notes to predefined ''circles.'' Google+ circles consist of other users and can be private, supporting a personal collection of notes, or include a selection of followers who will receive notifications when a new ''discovery note'' is posted.

Thus, this work explores a new paradigm for the publication of results from systems studies. The vast amounts of data generated when profiling immune response on a large scale often remain ''hidden'' behind the main results presented in a manuscript. Furthermore, when primary data is deposited in public repositories, it is often incomplete and is not readily accessible to investigators with limited bioinformatics expertise. Here, state-of-the-art application development was leveraged to provide readers with the opportunity to interact with the data underpinning each figure. We employed Web 2.0 concepts to build applications that support dynamically updated page content and the performance of computationally intensive tasks on a remote server (in this instance, on a cloud server) without the need for downloading or installing new software. Making data available via such web applications improves the transparency of the results. In addition, bridging the gap between investigators possessing vast immunological expertise and the large amounts of data generated in the context of systems profiling studies will promote further insights and knowledge discovery.

EXPERIMENTAL PROCEDURES

Study Subjects and Study Design

The study was approved by the Baylor Research Institute Institutional Review Board at Baylor University Medical Center (Dallas, TX). After obtaining written informed consent, healthy adults, aged 18 to 64 years, were enrolled to receive a single intramuscular dose of 2009–2010 seasonal influenza (Fluzone, Sanofi Pasteur, PA), pneumococcal vaccine (Pneumovax23, Merck, NJ), or placebo (saline). Exclusion criteria were pregnancy, active allergy symptoms, or vaccinations within the previous 2 months. Prior to vaccination, participants had two baseline blood draws (on days −7 and 0, with respect to the day of vaccination; see Tables S1 and S2 for study design). Blood was collected in Tempus blood RNA tubes (Life Technologies) for microarray and acid citrate dextrose tubes (ACD, BD Vacutainer) for whole-blood flow cytometry, CBC, and serum analysis of neutralizing antibodies (Figure S1) and cytokines (Figure S4). In addition, capillary blood was collected by finger stick for microarray (see Table S5 for study design). Freshly ficolled PBMC were used for sequential isolation of white blood cell subsets (see below).

Microarray Assay

Total RNA was isolated from the whole-blood lysate (Ovcharenko et al., 2005) followed by depletion of globin messenger RNA (Whitley et al., 2005). All samples passing quality control were then amplified and labeled by using the Illumina TotalPrep-96 RNA amplification kit. Amplified RNA was hybridized to Illumina HT-12 V3 beadchips (48,803 probes) and scanned on an Illumina Beadstation 500. Illumina's BeadStudio version 2 software was used to generate signal-intensity values from the scans. After background subtraction, the average normalization recommended by the BeadStudio 2.0 software (Illumina, San Diego, CA) was used to rescale the difference in overall intensity to the median average intensity for all samples across multiple arrays and chips. For modular analysis, a set of 260 transcriptional modules was used as a pre-existing framework for the analysis of this data set. The approach used for the construction of such framework was previously reported (Chaussabel et al., 2008). Briefly, genes with coordinate expression within or across nine whole-blood disease data sets where selected in multiple rounds of clique and paraclique clustering to form a 260 transcriptional module framework (see also Supplemental Experimental Procedures). Following the transformation of gene level data into module level activity scores, both unsupervised and supervised analyses of the complete data set were conducted.

Flow Cytometry

We incubated 200 uL of whole blood with pretitrated monoclonal antibodies for 15 min at room temperature followed by lysis of red blood cells (BD FACS Lyse). Samples were processed within 2 hr after blood draw and acquired on a BD Special Order LSRII flow cytometer. Analysis was performed by using FlowJo software (version 8.8.6, TreeStar, Inc.).

Isolation of WBC Subsets

Neutrophils were first separated from mononuclear cells by Ficoll gradient centrifugation, followed by hypotonic lysis of red blood cells in $KHCO_3$ and NH_4Cl and finally purified by negative selection by using the EasySep Human Neutrophil Enrichment Kit (Stemcell); monocytes ($CD14^+$) and T lymphocytes positive for the CD4 and CD8 antigen were sequentially isolated from PBMC by using Dynabeads (Invitrogen) according to the manufacturer's instructions.

In Vitro Stimulation with Innate Immune Ligands

Fresh whole blood of four healthy subjects was incubated for 6 hr at 37°C with 18 different stimuli or left unstimulated and followed by RNA stabilization with Tempus reagent and sample storage at −20°C until RNA extraction, as

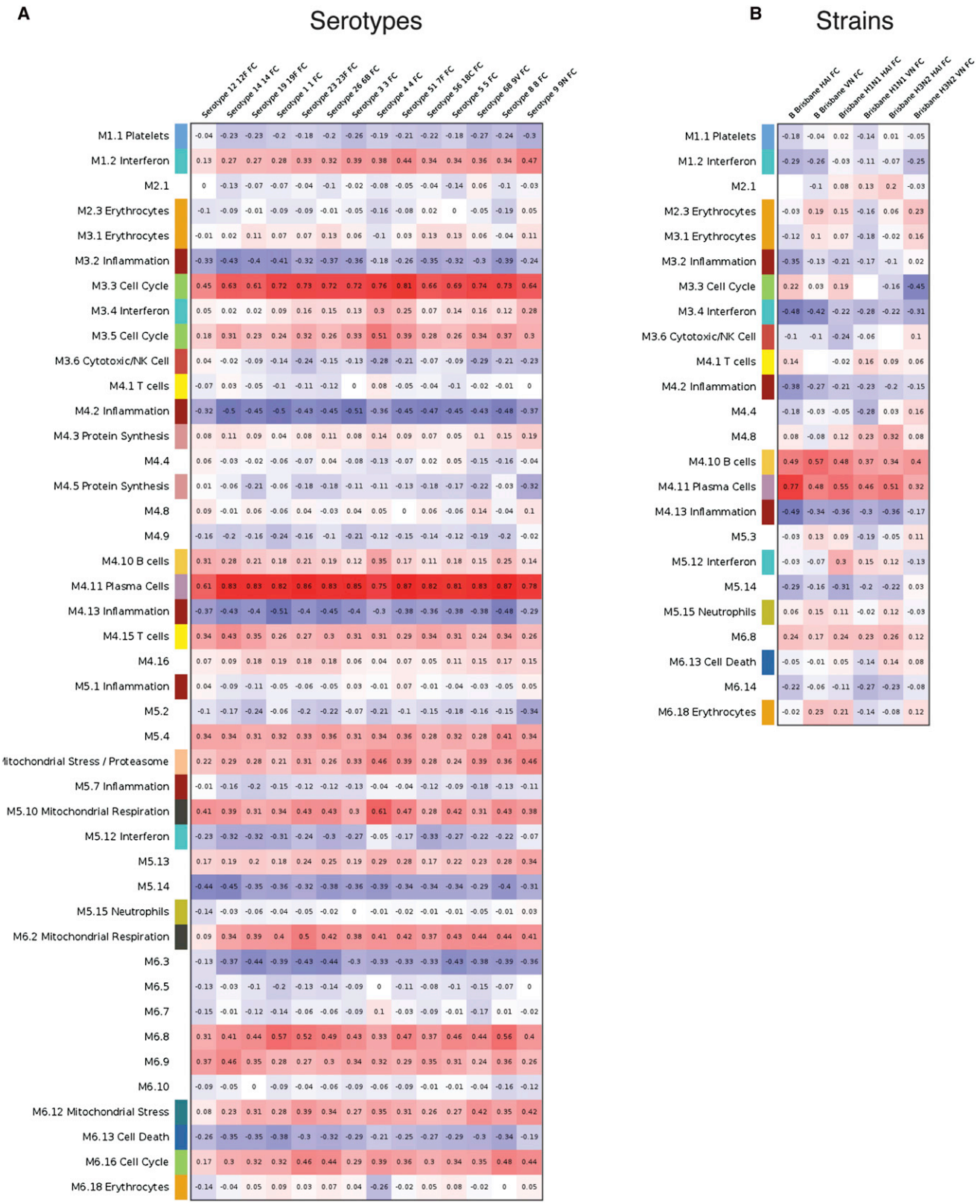

Figure 7. Correlation Patterns of Day 7 Transcriptional Data and Antibody Titers

Correlations between day 7 baseline-normalized averaged modular expression profiles and fold change of day 28 antibody titer over baseline for all available pneumococcal serotypes and influenza vaccine strains are represented on a heatmap. Modules are shown in rows and serotypes in columns. Red indicates

(legend continued on next page)

described above. Stimulation conditions included PAM3, Zymosan, Poly IC, E-LPS, Flagellin, R837, CpG Type A, heat-killed *Legionella pneumophila* (HKLP), heat-killed *Acholeplasma laidlawii* (HKAL), and heat-killed *Staphylococcus aureus* (HKSA) (all from Invivogen); IL-18, TNF-α, IFN-α2b, IFN-β, IFN-γ (all from Peprotech); heat-killed *Escherichia coli* (in house preparation), live influenza A virus and live respiratory syncytial virus (RSV).

Hemagglutinin Inhibition and Virus-Neutralization Assays for Quantitating Seasonal Influenza Virus Neutralizing Antibodies

Briefly, 2-fold serial dilutions of human sera were mixed and preincubated in 96-well plates for 30 min at room temperature with 8 hemagglutinin units of virus (H1N1 A/Brisbane/59/2007 and H3N2 A/Brisbane/10/2007) per well. Turkey red blood cells were used for detection of neutralizing antibodies against H3N2 A/Brisbane/10/2007, whereas chicken red blood cells were used or detection of neutralizing antibodies against H1N1 A/Brisbane/59/2007. Red blood cells were added at a final concentration of 0.25% per well, and the plate was incubated at room temperature for 30 min. Neutralizing antibody titers were determined as the reciprocal value of the highest dilution that displayed no hemagglutinating activity. Virus-neutralization assays were performed by using the same virus strains and as reported earlier (Steel et al., 2009). Antibody response to 14 pneumococcal polysaccharides was measured by using commercial immunoassays.

Multiplex Cytokine Analysis

Sera were analyzed for cytokine production by using the Multiplex 42-human cytokine and chemokine panel of antibodies conjugated beads and biotin pairs (Cf. Luminex Technology, Millipore) according to the manufacturer's instructions and run on Bio-Plex 200 and Bio-Plex 100 readers (Bio-Rad Laboratories).

Statistical Methods

Background-subtracted microarray data were obtained from Illumina's GenomeStudio software. Expression values less than 10 were set to 10, log (base 2) transformed, and quantile normalized. For flow data processing, all continuous outcome variables were log (base 2) transformed to better meet the normality assumption of the linear mixed model (LMM) analyses. Both microarray- and flow cytometry-derived variables were analyzed by using LMMs, which included time as a categorical variable with a first-order autoregressive residual covariance matrix. Specific contrasts were used to test for differences between postvaccination and both prevaccination time points. When applicable, differences between the two prevaccination time points were also tested as a control. A FDR of 0.10 was used to adjust for multiple testing (Benjamini and Hochberg, 1995). For each vaccine study in cohort 1, microarray probes were modeled individually. The number and proportion of differentially expressed probes (both up and downregulated) was determined per module and time point comparison. Modules containing a proportion of probes greater than an FDR of 0.10 were considered active at the specified time point and further investigated. The results in cohort 1 were validated in subsequent cohorts. The mean of all probes within a module was calculated for each observation and analyzed by using the same LMM as previously described. Statistical analyses of microarray, Luminex, flow cytometry, and serology data were performed by using SAS software (v9.2), JMP (v8), and JMP/Genomics (v4.0) (each from SAS Institute, NC).

Generation of Circular Plots

The in vivo vaccine response data sets were processed as described above. The in vitro stimulation data set was preprocessed by using quantile normalization and flooring all values to 10. Probes that did not have a detection p value < 0.01 in at least 10% of all samples across all stimuli and donors were excluded. For each stimulation, probes were identified with a fold change of greater than 2 or less than 0.5, when compared to the respective nonstimulated donors. Probes were identified separately for each stimulation and had absolute value difference >100 when compared to the nonstimulated donors. Finally, for each stimulation, probes were identified for which at least 3 samples passed both the fold change and signal difference threshold cutoff.

ACCESSION NUMBERS

Data have been deposited in the NCBI Gene Expression Omnibus under code GSE30101.

SUPPLEMENTAL INFORMATION

Supplemental Information includes four figures, six tables, and Supplemental Experimental Procedures and can be found with this article online at http://dx.doi.org/10.1016/j.immuni.2012.12.008.

ACKNOWLEDGMENTS

We thank our volunteer participants and all of the members of BIIR who assisted in this work. We thank I. Berthier, C. Boudreaux, A. Cobb, M. Hughes, B. Lemoine, I. Munagala, D. Nattamai, and colleagues for providing technical assistance with sample preparation, microarray processing, and flow cytometry. We thank A. Garcia-Sastre and R. Albrecht, Department of Microbiology, Mount Sinai School of Medicine, for advice and performing serological assays. We thank E. De Vol, N. Baldwin, and E. Whalen for advice and support in biostatistics and bioinformatics, G. Hayward for help depositing microarray data, M. Roy and O. Vargas for help with editing the wiki site, C. Samuelsen for organizational support, and R. Coffman for discussion of the manuscript. G.O. was supported by an Erwin Schrodinger Research Grant of the Austrian Science Fund and the Medical Research Fund MFF Tirol. The work of D.C., J.B., and K.P. are supported by the Baylor Health Care System Foundation and the National Institutes of Health (U19 AI08998, U19 AI057234, U01 AI082110, N01-AI-15416, and P01 CA084512). J.B., K.P., and D.C. designed the study; G.O., Y.W., E.A., L.T.-S., R.R., E.R, J.S., L.A., M.S., H.D., P.N., Q.-A.N., and S.M.Z. assisted in experiments; H.U. and V.P. supervised the experiments; A.C.H. recruited volunteers; G.O., H.X., Y.W., E.A., A.C., and D.B. analyzed the data; S.P., K.D., B.Z., A.B., D.A., C.S., E.I., G.T.N., and C.Q. provided bioinformatic tools and support, and G.O, K.P., and D.C prepared the manuscript.

Received: September 7, 2011
Accepted: December 21, 2012
Published: April 18, 2013

REFERENCES

Alakulppi, N., Seikku, P., Jaatinen, T., Holmberg, C., and Laine, J. (2008). Feasibility of diagnosing subclinical renal allograft rejection in children by whole blood gene expression analysis. Transplantation *86*, 1222–1228.

Benjamini, Y., and Hochberg, Y. (1995). Controlling the False Discovery Rate: A Practical and Powerful Approach to Multiple Testing. J.R. Stat. Soc. *57*, 289–300.

Bennett, L., Palucka, A.K., Arce, E., Cantrell, V., Borvak, J., Banchereau, J., and Pascual, V. (2003). Interferon and granulopoiesis signatures in systemic lupus erythematosus blood. J. Exp. Med. *197*, 711–723.

Berry, M.P., Graham, C.M., McNab, F.W., Xu, Z., Bloch, S.A., Oni, T., Wilkinson, K.A., Banchereau, R., Skinner, J., Wilkinson, R.J., et al. (2010). An interferon-inducible neutrophil-driven blood transcriptional signature in human tuberculosis. Nature *466*, 973–977.

strong positive correlation, and blue indicates strong negative correlation. (A) shows pneumococcal vaccine, and (B) shows influenza vaccine (D28/baseline fold change [FC] in virus neutralization [VN] and hemagglutinin [HAI] titers). An interactive supplement is available for this figure that allows users to dynamically filter modules and select additional parameters for correlation (iFigure 7: http://www.interactivefigures.com/dm3/vaccine-paper/figure-7.gsp). Correlations and associated p values were calculated via the Spearman method and can be adjusted by using a slider; Benjamini-Hochberg multiple testing correction is controlled by an on/off toggle. For details on serological response, see also Figure S1 and Tables S3 and S4.

Bucasas, K.L., Franco, L.M., Shaw, C.A., Bray, M.S., Wells, J.M., Niño, D., Arden, N., Quarles, J.M., Couch, R.B., and Belmont, J.W. (2011). Early patterns of gene expression correlate with the humoral immune response to influenza vaccination in humans. J. Infect. Dis. *203*, 921–929.

Caskey, M., Lefebvre, F., Filali-Mouhim, A., Cameron, M.J., Goulet, J.P., Haddad, E.K., Breton, G., Trumpfheller, C., Pollak, S., Shimeliovich, I., et al. (2011). Synthetic double-stranded RNA induces innate immune responses similar to a live viral vaccine in humans. J. Exp. Med. *208*, 2357–2366.

Chaussabel, D., Quinn, C., Shen, J., Patel, P., Glaser, C., Baldwin, N., Stichweh, D., Blankenship, D., Li, L., Munagala, I., et al. (2008). A modular analysis framework for blood genomics studies: application to systemic lupus erythematosus. Immunity *29*, 150–164.

Chaussabel, D., Ueno, H., Banchereau, J., and Quinn, C. (2009). Data management: it starts at the bench. Nat. Immunol. *10*, 1225–1227.

FDA (2011). Complete List of Vaccines Licensed for Immunization and Distribution in the US. http://www.fda.gov/BiologicsBloodVaccines/Vaccines/ApprovedProducts/ucm093833.htm.

Gaucher, D., Therrien, R., Kettaf, N., Angermann, B.R., Boucher, G., Filali-Mouhim, A., Moser, J.M., Mehta, R.S., Drake, D.R., 3rd, Castro, E., et al. (2008). Yellow fever vaccine induces integrated multilineage and polyfunctional immune responses. J. Exp. Med. *205*, 3119–3131.

Germain, R.N., Meier-Schellersheim, M., Nita-Lazar, A., and Fraser, I.D. (2011). Systems biology in immunology: a computational modeling perspective. Annu. Rev. Immunol. *29*, 527–585.

Maecker, H.T., McCoy, J.P., and Nussenblatt, R. (2012). Standardizing immunophenotyping for the Human Immunology Project. Nat. Rev. Immunol. *12*, 191–200.

Mallory, R.M., Malkin, E., Ambrose, C.S., Bellamy, T., Shi, L., Yi, T., Jones, T., Kemble, G., and Dubovsky, F. (2010). Safety and immunogenicity following administration of a live, attenuated monovalent 2009 H1N1 influenza vaccine to children and adults in two randomized controlled trials. PLoS ONE *5*, e13755.

Nakaya, H.I., Wrammert, J., Lee, E.K., Racioppi, L., Marie-Kunze, S., Haining, W.N., Means, A.R., Kasturi, S.P., Khan, N., Li, G.-M., et al. (2011). Systems biology of vaccination for seasonal influenza in humans. Nat. Immunol. *12*, 786–795.

Ovcharenko, D., Jarvis, R., Hunicke-Smith, S., Kelnar, K., and Brown, D. (2005). High-throughput RNAi screening in vitro: from cell lines to primary cells. RNA: A Publication of the RNA Society *11*, 985–993.

Pascual, V., Chaussabel, D., and Banchereau, J. (2010). A genomic approach to human autoimmune diseases. Annu. Rev. Immunol. *28*, 535–571.

Querec, T.D., Akondy, R.S., Lee, E.K., Cao, W., Nakaya, H.I., Teuwen, D., Pirani, A., Gernert, K., Deng, J., Marzolf, B., et al. (2009). Systems biology approach predicts immunogenicity of the yellow fever vaccine in humans. Nat. Immunol. *10*, 116–125.

Ramilo, O., Allman, W., Chung, W., Mejias, A., Ardura, M., Glaser, C., Wittkowski, K.M., Piqueras, B., Banchereau, J., Palucka, A.K., and Chaussabel, D. (2007). Gene expression patterns in blood leukocytes discriminate patients with acute infections. Blood *109*, 2066–2077.

Steel, J., Lowen, A.C., Pena, L., Angel, M., Solórzano, A., Albrecht, R., Perez, D.R., García-Sastre, A., and Palese, P. (2009). Live attenuated influenza viruses containing NS1 truncations as vaccine candidates against H5N1 highly pathogenic avian influenza. J. Virol. *83*, 1742–1753.

Tang, B.M., McLean, A.S., Dawes, I.W., Huang, S.J., and Lin, R.C. (2009). Gene-expression profiling of peripheral blood mononuclear cells in sepsis. Crit. Care Med. *37*, 882–888.

Whitley, P., Moturi, S., Santiago, J., Johnson, C., and Setterquist, R. Ambion, Inc. (2005). Improved Microarray Sensitivity using Whole Blood RNA Samples. In Applied Biosystems TechnicalNotes.

Wrammert, J., Smith, K., Miller, J., Langley, W.A., Kokko, K., Larsen, C., Zheng, N.-Y., Mays, I., Garman, L., Helms, C., et al. (2008). Rapid cloning of high-affinity human monoclonal antibodies against influenza virus. Nature *453*, 667–671.